Published in final edited form as:
Sci Transl Med. 2011 October 5; 3(103): 103ra97. doi:10.1126/scitranslmed.3002627.

Increased Gene Dosage of *Ube3a* Results in Autism Traits and Decreased Glutamate Synaptic Transmission in Mice

Stephen E. P. Smith[1], **Yu-Dong Zhou**[1], **Guangping Zhang**[1], **Zhe Jin**[1], **David C. Stoppel**[1,2], and **Matthew P. Anderson**[1,2,*]

[1]Beth Israel Deaconess Medical Center, Departments of Pathology and Neurology, Harvard Medical School, Boston, MA 02215, USA

[2]Program in Neuroscience, Harvard Medical School, Boston, MA 02215, USA

Abstract

People with autism spectrum disorder are characterized by impaired social interaction, reduced communication, and increased repetitive behaviors. The disorder has a substantial genetic component, and recent studies have revealed frequent genome copy number variations (CNVs) in some individuals. A common CNV that occurs in 1 to 3% of those with autism—maternal 15q11-13 duplication (dup15) and triplication (isodicentric extranumerary chromosome, idic15)—affects several genes that have been suggested to underlie autism behavioral traits. To test this, we tripled the dosage of one of these genes, the ubiquitin protein ligase *Ube3a*, which is expressed solely from the maternal allele in mature neurons, and reconstituted the three core autism traits in mice: defective social interaction, impaired communication, and increased repetitive stereotypic behavior. The penetrance of these autism traits depended on *Ube3a* gene copy number. In animals with increased *Ube3a* gene dosage, glutamatergic, but not GABAergic, synaptic transmission was suppressed as a result of reduced presynaptic release probability, synaptic glutamate concentration, and postsynaptic action potential coupling. These results suggest that *Ube3a* gene dosage may contribute to the autism traits of individuals with maternal 15q11-13 duplication and

*To whom correspondence should be addressed. Matthew_Anderson@bidmc.harvard.edu.

Author contributions: M.P.A., S.E.P.S., and Y.-D.Z. designed the study. M.P.A. and S.E.P.S. wrote the paper. S.E.P.S., Y.-D.Z., G.Z., and M.P.A. analyzed the data. S.E.P.S. did behavioral and protein studies. Y.-D.Z. performed all electrophysiology experiments except miniature postsynaptic currents and action potential coupling experiments done by G.Z. Z.J. engineered the BAC constructs. D.C.S. did the synaptic density measures.

Competing interests: The authors declare that they have no competing interests. A patent has been filed by Beth Israel Deaconess Medical Center on the animal model of autism reported in this paper with M.P.A. as inventor.

SUPPLEMENTARY MATERIAL
www.sciencetranslationalmedicine.org/cgi/content/full/3/103/103ra97/DC1
Material and Methods
Fig. S1. Recombineering a C-terminal FLAG tag into the three isoforms of the wild-type Ube3a gene (162 kb, BAC vector).
Fig. S2. Design and expression of *Ube3a* BAC transgene.
Fig. S3. Distribution of transgenic and native Ube3a protein expression in the brain.
Fig. S4. Gender-specific effects of increased *Ube3a* gene dosage on social, repetitive, and communication behaviors.
Fig. S5. Effects of increased *Ube3a* gene dosage on developmental milestones.
Fig. S6. Effects of increased *Ube3a* gene dosage on spontaneous EPSCs, spontaneous IPSCs, and mEPSCs at −80 mV in layer 2/3 pyramidal neurons from the barrel cortex.
Fig. S7. Effects of increased *Ube3a* gene dosage on release probability, readily releasable pool size, and AMPA and NMDA kinetics.
Fig. S8. Effects of increased *Ube3a* gene dosage on synaptic and other neuronal proteins.
Fig. S9. Effects of increased *Ube3a* gene dosage on quantity of proteins regulating synaptic glutamate concentration.
Fig. S10. Effects of increased *Ube3a* gene dosage on other biophysical properties of layer 2/3 barrel cortex pyramidal neurons.
Table S1. Effects of increased *Ube3a* gene dosage on behavior: statistical analyses. References

support the idea that increased E3A ubiquitin ligase gene dosage results in reduced excitatory synaptic transmission.

INTRODUCTION

Autism spectrum disorders (ASDs) are estimated to affect 1 in 110 individuals and are clinically defined by three core traits: impaired social interaction, reduced communication, and increased repetitive, stereotyped behaviors (1). Despite high heritability revealed by sibling, twin, and family studies (2), the diagnosis is based solely on behavioral criteria. The phenotypic heterogeneity and frequent medical comorbidities that characterize the disorder also present significant challenges for animal modeling and translational research. Existing mouse models of syndromic neurodevelopmental disorders such as Rett syndrome, fragile X, and tuberous sclerosis have proven invaluable for investigations of these specific conditions, but these conditions display incomplete autism penetrance and include other neurologic and pathologic comorbidities.

Recent studies have established the presence of a high rate of small genomic DNA copy number variations (CNVs) in ASD, present in 10 to 20% of cases (3–7). The altered gene dosages resulting from these CNVs may explain a significant proportion of autism cases. Maternally inherited 15q11-13 duplications and triplications are among the most common genomic CNVs identified in patients with autism (1 to 3%) (3, 8). Individuals with one extra maternal 15q11-13 copy, inverted duplication (dup15), display partial autism penetrance, whereas individuals with two extra copies resulting from an isodicentric extra-numerary chromosome (idic15) display near-complete autism penetrance (8). Paternally inherited duplications (with rare exceptions) are not associated with autism (8). These observations suggested to us that the dosage of an imprinted gene or genes within the duplicated region underlies the autism risk in these patients.

E3 ubiquitin-protein ligase, *Ube3a* (also known as E6-AP), is the only gene within the 15q11-13 duplicated segment consistently expressed solely from the maternal allele in mature neurons (9), making it a likely candidate to mediate the autism phenotype. CNVs of other E3 ligase genes have recently been identified in ASD (3). Moreover, inactivating mutations or deletions of *Ube3a* cause Angelman syndrome, a neurological disorder characterized by intellectual disability, hypotonia, and seizures (10, 11).

The *Ube3a* imprinting seen in humans is preserved in mice, and inheritance of a maternal allele deletion is sufficient to reconstitute many of the features of Angelman syndrome including seizures, defective motor performance, impaired contextual fear learning, defective synaptic long-term potentiation, and reduced dendritic spine density (10, 12, 13). The molecular mechanisms by which Ube3a deficiency in Angelman syndrome causes cognitive impairments are not fully understood. Nevertheless, the Angelman mouse model displays a significant increase in the phosphorylation of hippocampal α-calcium/calmodulin-dependent protein kinase II (αCaMKII), specifically at the constitutively active site Thr^{286} and the autoinhibitory site Thr^{305} (14, 15). Furthermore, by crossing the Angelman mouse model to mice with an αCaMKII-T305V/T306A mutant knock-in that prevents inhibitory autophosphorylation of αCaMKII, the incidence of seizures was decreased, and the deficits in motor function, learning, and synaptic plasticity were partially reversed (15). More recently, the Angelman mouse model was shown to display impaired experience-dependent maturation of visual cortex, and defects in synaptic plasticity were rescued by dark rearing (16, 17). However, the proteins ubiquitinated by Ube3a that might mediate these behavioral and synaptic defects have not been identified. Ube3a (E6-AP) was originally discovered to ubiquitinate and promote degradation of p53, through which it plays a pathogenic role in human papillomavirus–induced cervical epithelium neoplasia (18).

More recently, Ube3a was shown to ubiquitinate and promote degradation of two important neuronal proteins: Arc and Ephexin5 (19, 20).

On the basis of these effects of maternal *Ube3a* deficiency on behavior and neuronal function, we hypothesized that increased *Ube3a* dosage in individuals with 15q11-13 duplication might underlie autism behavioral traits. Thus, we predicted that increased *Ube3a* gene dosage might produce autism-related behavioral traits in mice. Because autism behavioral traits are weakly penetrant in individuals with dup15, but highly penetrant in idic15 (8), we compared these traits in mice with a doubling or tripling of the normal *Ube3a* gene dosage expressed in mature neurons, aimed at modeling dup15 and idic15, respectively.

RESULTS

Genetically increasing *Ube3a* gene copy number increases protein levels

We hypothesized that *Ube3a* mediates the autism-related behavioral phenotypes associated with dup15 and idic15 because of its known roles in neurologic function and because *Ube3a* is the only gene in the region known to be expressed exclusively from the maternal chromosome (Fig. 1A). Using bacterial artificial chromosome (BAC) recombineering techniques (21), we inserted a 162-kb segment of mouse chromosome 7 (syntenic to human chromosome 15), containing the entire 78-kb exon-intron coding sequence of Ube3a as well as its 63-kb 5′ and 21-kb 3′ extragenic sequences, into FVB embryos to generate transgenic mice, which were subsequently bred to produce single (1×Tg) and double (2×Tg) copy transgenic animals. A 3×FLAG tag followed by two stop codons was inserted in-frame in exon 12 [isoforms 2 and 3, long form (L)] or in exon 8 [isoform 1, short form (S)] to produce the full-length FLAG-tagged transgenic protein (figs. S1 and S2A). Transgenic mice carrying the exon 12 FLAG insert (isoforms 2 and 3, L) are used throughout the paper, unless otherwise noted. Two independent transgenic founder lines of the exon 12 insert (L) with independent integration sites were compared to control for any potential insertion-site effects (Ube3a, founder lines 1 and 2); line 1 is used throughout, except where otherwise noted.

Ube3a 1× and 2× transgenic mice were identified by semiquanti-tative polymerase chain reaction (PCR) (fig. S2B) and confirmed by Western blot to express two and three times more Ube3a protein in whole-brain lysates than wild-type mice, respectively (Fig. 1B). The endogenous *Ube3a* gene is expressed only from the maternal chromosome in neurons, explaining this dose-dependent effect of adding extra *Ube3a* copies. But the *Ube3a* transgene expresses independent of parent of origin as a result of the lack of the antisense transcript initiation site underlying imprinting (22) (fig. S2C). Transgene expression is also independent of sex (fig. S2D). We concluded that the *Ube3a* transgene generated functional protein because FLAG antibody immunoprecipitated long (L), but not short (S), FLAG-tagged Ube3a isoform degraded exogenous recombinant Arc, a known Ube3a target (19) in vitro (Fig. 1C). Further, *Ube3a* (2×) transgene decreased endogenous Arc in the barrel cortex (Fig. 1D). Immunofluorescence staining for FLAG in the Ube3a-FLAG transgenic animals recapitulated the native Ube3a staining pattern seen in wild-type animals and matched previously reported *Ube3a* expression patterns (17, 23) (fig. S3). Further, dual immunofluorescence staining to FLAG and Ube3a showed complete overlap in cortex, hippocampus, and thalamus, indicating that the transgenic protein expresses in all cells expressing native Ube3a (Fig. 1, E to G).

Increasing *Ube3a* gene dosage impairs social behavior

Impaired social interaction is a hallmark of autism. We assessed a measure of this trait in juvenile transgenic mice, using a three-chamber social interaction test (24) in which mice are first acclimated to the arena and then choose between a social chamber containing a caged and sex- and age-matched wild-type stranger mouse and a chamber with an empty cage (Fig. 2A). Wild-type mice displayed normal social preference, spending more time on the side of the apparatus containing the probe mouse (Fig. 2B) and more time interacting with the probe mouse (Fig. 2C). *Ube3a* transgenic mice with three times the normal amounts of Ube3a protein (2×Tg) failed to show a social preference in either measure, investigating the empty and mouse-occupied cages equally. *Ube3a* transgenic mice with twice the normal amount of Ube3a (1×Tg) showed an intermediate phenotype, failing to show a preference for the social zone but showing a significant preference to interact with the cage occupied by a mouse (Fig. 2, B and C). Comparisons across genotypes are not standard (24) but resulted in the same conclusions (table S1). Plotting the middle zone time as a function of genotype shows the preference for the outer two zones containing the novel objects (cages) in all strains (Fig. 2B). We then performed a different version of the three-chambered social interaction test on a new cohort of adult mice with acclimation of the mice to both the arena and the cages (Fig. 2D) (25). In this paradigm, wild-type and *Ube3a* (1×) transgenic mice displayed a more robust preference for the side containing the novel mouse (Fig. 2E). *Ube3a* (2×Tg) transgenic mice again showed no preference for the side containing the mouse, whether assessed as time in the social zone (Fig. 2E) or in close proximity to the probe mouse (Fig. 2F). Ube3a transgenic mice carrying two copies of the inactive short form (2×S) also displayed a normal social preference (Fig. 2, E and F, and table S1). This second social behavior experimental design permitted us to add a novel object rather than the probe mouse to the cage, revealing that *Ube3a* (2×Tg) transgenic mice, like controls, displayed a normal preference for this immobile novel object (Fig. 2G). Two independent *Ube3a* (2×Tg) transgenic founders (lines 1 and 2) displayed the same lack of preference for interaction with the novel mouse, eliminating transgene insertion effects (Fig. 2H). The *Ube3a* (2×Tg) transgene also abolished the social preference equally in males and females (fig. S4A).

One potential explanation for the lack of social preference could be motor deficits or increased generalized anxiety. However, in the open field test, *Ube3a* (2×) transgenic mice displayed mobility that was similar to that of controls (Fig. 3A). The number of entries into the center and time spent in the center of the field also did not differ from that of controls (Fig. 3, B and C); anxious mice tend to avoid the center space in an open field. In the elevated plus maze, *Ube3a* (2×) transgenic mice explored the open arms similar to controls (Fig. 3, D to F), again providing no evidence of an anxiety-like phenotype. Motor performance on the accelerating rotorod in adulthood was also similar across genotypes (Fig. 3G). Orienting motor responses during post-natal development were also unaffected (fig. S5). Finally, novel object exploration (Fig. 3, H and I) and short-term object memory (Fig. 3, H and J) were similar across genotypes. The results indicate that a tripling of *Ube3a* gene dosage impairs social interaction, a potential correlate of the social behavior deficits found in human autism, whereas a doubling of Ube3a gene dosage causes a more limited social behavior deficit only during competition between a mouse and a novel object.

Increasing *Ube3a* gene dosage impairs communication and increases repetitive behavior

Defective communication is the second diagnostic criteria of autism. Thus, we assessed whether increased *Ube3a* gene dosage impairs communicative ultrasonic vocalizations in mice (Fig. 4, A to D). We measured two types of social behavior–relevant vocalizations in adult rodents: vocalizations generated by same-sex pairs encountering each other for the first time and vocalizations generated by sexually experienced males exposed to female urine.

Social stimulus–induced vocalizations were assessed when two age-, sex-, and genotype-matched, nonlittermate stranger mice were paired. Wild-type mice emitted vocalizations that were markedly reduced by the 2×, but not the 1×, *Ube3a* transgene dosage (Fig. 4A). *Ube3a* 2× transgene effects were most pronounced in females, because female pairs vocalized with a much greater frequency than males (fig. S4). As previously reported (26), female urine elicited a diverse repertoire of vocalizations in sexually experienced, wild-type males (Fig. 4, B to D). In this test, the number of vocalizations and the time spent vocalizing were strongly reduced in both 1× and 2× *Ube3a* transgenic mice (Fig. 4B). Despite the large decrease of vocalization quantity, other vocalization features were unaffected: average peak frequency (67 ± 1, 67 ± 2, and 69 ± 2 kHz, respectively) and call type distribution (Fig. 3D). To control for a potential confounding deficit in olfaction, we tested mice in an olfactory habituation/dishabituation test, which confirmed the ability of transgenic animals to respond normally to novel scents presented on a cotton swab (Fig. 4E). There could also be a general deficit in the ability to vocalize. However, arguing against this possibility is the observation that pup vocalizations during a 5-min separation from their mother, an aversive stimulus (27), were unaffected by the increased *Ube3a* gene dosage (Fig. 4F). The results indicate that ultrasonic vocalizations generated in a social context are impaired by increases of *Ube3a* gene dosage.

The third hallmark autism trait is repetitive, stereotyped behaviors such as body rocking, hand flapping, or self-injurious behavior. These behaviors have been assumed to be equivalent to repetitive self-grooming in mice (24, 28, 29). Self-grooming was increased by three times in *Ube3a* (2×Tg) transgenic mice, but was unaffected in *Ube3a* (1×Tg) compared to wild types (Fig. 4G). We ruled out the possibility that these effects were caused by disruptions from the transgene insertion by showing that two independent Ube3a transgene founder lines 1 and 2 produced the same increase of self-grooming relative to that of control littermates (Fig. 4H). Increased self-grooming was also observed when male and female *Ube3a* (2×Tg) transgenic mice were separately examined (fig. S4). Transgenic mice carrying a 2× gene dosage of the enzymatically inactive *Ube3a* [the short (S) form] (2×S) exhibited normal grooming (Fig. 4G). In summary, tripling *Ube3a* gene dosage expressed in neurons caused impairment of all three measures of autistic-like behavior—decreased social interaction and vocalization and excessive repetitive grooming behavior. Doubling the Ube3a gene dosage caused a more limited phenotype in mice, selectively impairing social interactions during novel object competition (not prehabituated to the cages) and male vocalizations to a female urine stimulus.

Increased *Ube3a* gene dosage impairs glutamatergic synaptic transmission

Ube3a is present in the cytoplasm, the nucleus, and at distinct dendritic puncta colocalized with the synapse marker postsynaptic density protein 95 (PSD-95) in mouse cortical neuron primary cultures (fig. S3, I to Q). We hypothesized that increasing *Ube3a* gene dosage might alter evoked excitatory and/or inhibitory postsynaptic currents (EPSCs and IPSCs) in cortical pyramidal neurons. We measured somatosensory whisker barrel cortex layer 2/3 pyramidal neurons, because the neurons are highly active [Ube3a is an activity-induced gene (19)], strongly express Ube3a (Fig. 1F and fig. S3, A and B) (19, 23), and have been previously studied in other mouse models of ASD. These neurons reportedly displayed increased GABAergic transmission in a mouse carrying the autism-associated neuroligin 3 (*NLGN3*) point mutation (30) and decreased GABAergic transmission because of GABAergic neuron deletion in the MeCP2 mouse model of Rett syndrome (31) without affecting glutamatergic synaptic transmission.

Synaptic currents were measured by whole-cell, voltage-clamp recordings in acute brain slices. Slices from *Ube3a* (2×Tg) transgenic mice displayed strong suppression of EPSC amplitude (Fig. 5A). By contrast, IPSC amplitude was not significantly reduced (Fig. 5B).

We measured spontaneous IPSCs and EPSCs and found reduced spontaneous EPSC amplitude and frequency (fig. S6A). Spontaneous IPSCs had reduced amplitudes but unaltered frequencies (fig. S6B). Thus, increasing *Ube3a* gene dosage markedly reduced glutamatergic synaptic transmission but had more limited effects on GABAergic transmission.

To address the mechanism of this effect, we recorded miniature EPSCs (mEPSCs) and miniature IPSCs (mIPSCs), with action potentials inhibited. *Ube3a* (2×) strongly suppressed mEPSC amplitude and frequency (Fig. 5C). By contrast, and unlike the *Nlgn3* and *Mecp2* mutant mice (30, 31), excess *Ube3a* failed to significantly alter mIPSC frequency or amplitude (Fig. 5D). To be sure that the reduced mEPSC frequency was not a result of reduced mEPSC amplitude (falling below detection threshold), we clamped the cells at −80 mV to increase amplitude. Again, we found reduced mEPSC amplitude and frequency (fig. S6C). These decreases in mEPSC amplitude, typically due to reduced postsynaptic AMPA receptors, and the decreased mEPSC frequency, typically due to reduced synapse number or presynaptic release probability, suggested that increased *Ube3a* gene dosage may regulate glutamate synaptic transmission at both pre- and post-synaptic sites.

Increasing Ube3a gene dosage reduces presynaptic glutamate release via two mechanisms

Synaptic glutamate release (R) is governed by the equation $R = Npq$, where N is the number of release sites, p is the probability of release, and q is the quantal size. We suspected that a change in synapse number might contribute to the decreased glutamate release, a mechanism analogous to the maternal *Ube3a* knockout mice that displayed fewer dendritic spines (12, 17). Therefore, we looked for changes in glutamate synapse number in layer 2/3 barrel cortex using three independent measures: counting asymmetric synapses using electron microscopy (Fig. 6A); counting the number of puncta with colocalized pre- and postsynaptic markers, VGlut1 and PSD-95, in thin (5 μm) sections by dual immunofluorescence staining (Fig. 6B); and counting dendritic spines in Golgi-stained sections (Fig. 6C). By all measures, synapse number was unaltered by the increased *Ube3a* (2×) gene dosage. Furthermore, the number of release sites, assessed electro-physiologically (see below), was unaltered (fig. S7). Thus, changes in N failed to explain the reduced mEPSC frequency.

Presynaptic release probability (p), another potential cause of decreased mEPSC frequency, was assessed with a repeated minimum stimulation protocol (fig. S7, A to D). Release probability was significantly reduced in *Ube3a* (2×) transgenic mice (fig. S7D). Paired-pulse ratio, increased at low-release probability synapses, was also increased in *Ube3a* (2×) transgenic mice (Fig. 7A). Both measures suggested that increasing *Ube3a* gene dosage decreases the release probability (p) of cortical glutamate synapses and so reduced mEPSC frequency, contributing to the lowered efficacy of glutamatergic synaptic transmission.

Quantal size (q) can be altered by pre- or post-synaptic changes, and reduced mEPSC amplitude often results from decreased postsynaptic AMPA receptor density. To directly measure the postsynaptic glutamate receptor responses, we applied small puffs of glutamate to the neuron and recorded postsynaptic AMPA and *N*-methyl-D-aspartate (NMDA) currents. Glutamate iontophoresis induced AMPA and NMDA receptor currents that were similar in amplitude across genotypes (Fig. 6D). In separate experiments, fiber stimulation–evoked AMPA and NMDA currents displayed a similar NMDA/AMPA ratio (Fig. 6E). Using antagonists to isolate mEPSC AMPA or NMDA currents, we showed that the decay time kinetics of these currents did not differ among genotypes (fig. S7, E and F), revealing no evidence of altered receptor subunit composition. Additionally, the quantity of glutamate receptor subunits and other synaptic proteins, when measured by Western blot of microdissected barrel cortex, were unaltered (fig. S8). The results suggested that *Ube3a* does

not reduce glutamatergic synaptic transmission and quantal size (*q*) by decreasing the number of postsynaptic AMPA or NMDA glutamate receptors.

The reduced mEPSC amplitude with preserved postsynaptic glutamate receptor function suggested a possible decrease in synaptic glutamate concentration. To test this hypothesis, we applied a weak glutamate receptor antagonist, γ-DGG (γ-D-glutamylglycine), to assess for a glutamate concentration–dependent decrease of synaptic transmission. A greater percent inhibition by γ-DGG indicates a lower synaptic glutamate concentration (32). γ-DGG did indeed reduce EPSC amplitude to a greater extent in *Ube3a* (2×) transgenic than in wild-type neurons, indicating that increased *Ube3a* gene dosage decreased synaptic glutamate concentration (Fig. 7B). The decreased synaptic glutamate could not be explained by reduced synaptic vesicle diameter [measured by electron microscopy: wild type, 37.40 ± 0.22 nm; *Ube3a* (2×), 37.37 ± 0.19 nm] or reduced glutamate transporter protein (VGlut1 or EAAT1-3) (fig. S9).

Ube3a reduces postsynaptic excitability to phasic excitatory synapse-like stimuli

Effective glutamatergic synaptic transmission also depends on the efficacy with which EPSCs couple to the firing of postsynaptic action potentials. This EPSC-spike coupling was assessed with short (5 ms) EPSC-like current injections directly into the patch-clamped neuron, bypassing the defects already shown to be present at the synaptic inputs. This measure assesses the intrinsic excitability of a neuron, compared to the EPSC measures, which assess synaptic inputs from surrounding neurons. *Ube3a* (2×) transgenic mice displayed impaired ES coupling (Fig. 7C). By contrast, action potential threshold, capacitance, and resting membrane potential were unaltered, whereas peak firing rate showed some evidence of a decrease (fig. S10). The results indicate that in addition to the strong impairment of glutamatergic synaptic transmission, the ability of these synaptic currents to couple to the firing of a postsynaptic action potential is concurrently suppressed by increased *Ube3a* gene dosage.

In summary, excess Ube3a acts at multiple, distinct sites within the pre- and postsynaptic compartments of the neuronal circuitry to impair excitatory synaptic transmission, causing decreased presynaptic vesicle release probability, decreased synaptic glutamate concentration, and decreased postsynaptic EPSC-spike coupling. By contrast, glutamate synapse densities and postsynaptic glutamate receptors were unaltered and GABAergic synaptic transmission showed only minor changes.

DISCUSSION

To date, several ASD mouse models—based on rare single gene point mutations [for example, NLGN3 (30, 33) and Shank3 (34–37)], syndromic disorders with partial autism penetrance [for example, tuberous sclerosis, fragile X, and Rett syndrome; see (38, 39)], mouse social behavior screens [for example, BTBR mouse (40) and MALTT mouse (41)], or immune models (25, 42)—have phenocopied a subset of the behavioral components of ASD. Our mouse model of ASD with extra copies of the *Ube3a* gene, which was designed to reproduce in part a common known risk factor for ASD (15q11-13 duplication present in 1 to 3% of ASD cases), displayed strong penetrance of three core autism-related behavior traits and to date has not displayed other major confounding traits or comorbidities [no evidence of the following: anxiety (elevated plus maze, open field test, social avoidance); motor behavior deficits (rotorod performance, motor milestones); memory deficits (object memory); or sensory behavior deficits (olfactory response, novel object recognition)].

Individuals with idic15 show typical autism traits such as reduced speech, reduced socialization including reciprocity and eye contact, and repetitive stereotyped behaviors.

There is also some evidence for regression in idic15 with better eye contact and vocalizations in infants and toddlers than in older children (8). There are also reports of delayed echolalia, pronoun reversal, and stereotyped utterances. A recently recognized feature of individuals with idic15 is comorbid epilepsy and sudden unexpected death in epilepsy (SUDEP) (8). Individuals with idic15 also display moderate to severe learning deficits that correlated in one study to the severity of the comorbid epilepsy (43). Our mice, which carry the idic15-equivalent increase in *Ube3a* gene dosage, showed behavioral correlates of the typical autism traits, but epilepsy and detailed learning and memory testing have not yet been performed.

We directly compared mice with *Ube3a* gene duplication and triplication and found gene-dosage effects on autism-related trait penetrance as observed in humans (8). Although gene dosage does not necessarily predict mRNA and protein dosage, studies in transformed idic15 lymphocytes and two idic15 postmortem brain samples indicate that the increase of Ube3a mRNA and protein is generally proportional to the increase of chromosomal gene dosage (44, 45). In our mice, a threefold increase of brain Ube3a protein, as would be predicted for patients with idic15, caused strong autism trait penetrance and reconstituted surrogates of all three core autism-related behavioral traits. By contrast, a twofold increase of brain Ube3a protein, as would be predicted for patients with dup15, associated with weaker autism penetrance and generated only a subset of the behavioral defects (most strongly reduced male vocalizations to female urine). These dose-dependent effects of increased *Ube3a* gene copies may explain the difficulty in finding autism traits in a recently developed mouse model aimed at reconstituting the maternally inherited autism disorder associated with dup15 (46). In this report, the authors used an elegant chromosome-engineering technique to replicate dup15 in mice (spanning the full set of genes within the syntenic region of chromosome 7) and demonstrated the expected maternal- and paternal-specific gene expression patterns of the imprinted chromosomal region. Yet, despite successful reconstitution of the typical expression pattern of Ube3a in brain tissues and the expected doubling of brain Ube3a mRNA when inheriting this duplication from the mother, autism-related behavioral traits were not observed with maternally inherited 15q11-13 duplications. Instead, they reported some behavioral deficits with paternally inherited 15q11-13 duplication. Our finding that a triplication of *Ube3a* gene dosage is necessary to reconstitute the full set of autism-like traits in mice may explain the lack of phenotype in this mouse model. Triplication of the maternally inherited *Ube3a* gene cannot be generated with this chromosome engineering technique, a limitation overcome by our BAC transgenic approach.

The 15q11-13 duplicated region contains at least 30 characterized genes, several previously proposed to underlie the autism phenotype. ATP10A is of interest because early studies suggested that, like Ube3a, it is expressed exclusively from the maternal chromosome (47, 48), although this has since been refuted (46, 49). Other genes within the duplicated genomic region, such as $GABA_A$ (γ-aminobutyric acid type A) receptor subunits $\beta 3$, $\alpha 5$, and $\gamma 3$ and cytoplasmic FMRP-interacting protein 1 (CYFIP1), have also been proposed to mediate the autism risk (8, 50). None are imprinted in a way that readily explains the selective association of autism with maternally inherited duplications, although their expression may be regulated in more complex, as yet undefined, ways (51). Although we cannot rule out a contribution from these other genes, our results indicate that increased dosage of the *Ube3a* gene alone is sufficient to replicate the three core autism-related traits in mice. Because our study did not systematically examine all possible genes within the 15q11-13 duplicated region, we cannot eliminate the possibility that increases or even decreases of expression of other genes could contribute.

The glutamatergic synaptic defects we report in these mice with increased *Ube3a* gene dosage are not those predicted from simply inverting the effects previously observed in the Angelman syndrome mouse model with a heterozygous, maternally inherited *Ube3a* knockout. For example, Yashiro *et al.* (17) reported that a loss of maternal Ube3a reduces mEPSC frequency in visual cortex layer 2/3 pyramidal neurons, an effect we also report with increased *Ube3a* gene dosage in comparable neurons of the somatosensory cortex. Similarly, Greer *et al.* (19) reported that a loss of maternal Ube3a reduces glutamatergic synaptic transmission, evoked AMPA/NMDA current ratio, and mEPSC amplitude in hippocampal CA1 pyramidal neurons. They attributed this effect to increases of the Ube3a target Arc that is known to regulate AMPA receptor trafficking and would deplete synaptic AMPA receptors when increased (52). Although we confirmed that increasing *Ube3a* gene dosage partially reduces Arc, the predicted increase in AMPA currents was not observed. Loss of maternal Ube3a was also reported to decrease dendritic spine density, potentially explaining the reduced mEPSC frequency reported in visual cortex (12, 17). Yet, increasing *Ube3a* gene dosage reduced mEPSC frequency, but did not increase or decrease dendritic spine density or glutamate synapse density. Although both high and low levels of *Ube3a* associate with human neurologic diseases, our findings suggest that the molecular and circuit mechanisms leading to Angelman syndrome and idic15 autism may be quite different.

Comparison of the circuit and behavioral defects in this *Ube3a* (2×) transgenic mouse model with those of other models of ASD may yield insights into shared pathophysiological mechanisms. A recently published report of a Shank3-deficient mouse model of ASD (36) indicated that the animals display increased anxiety (elevated plus maze), potentially explaining defective social interaction. In the three-chambered social interaction test, these mice avoided the chamber containing the probe mouse, consistent with reduced social interaction due to increased fear/anxiety. In contrast, our ASD mice with increased *Ube3a* gene dosage showed no evidence of anxiety behavior and did not avoid the social chamber side. Similarly, other mouse models including the Shank3 (36) and Angelman syndrome mice (10, 53) display impaired motor function on the accelerating rotorod, another potential behavioral confound. *Ube3a* (2×) transgenic mice displayed no defects in accelerating rotorod performance or other motor milestones. These differences further support the recognized heterogeneity of ASD.

Differences are also emerging in the types of circuit defects found in ASD mouse models. For example, mice with knock-in of an ASD-associated neuroligin 3 point mutation show increased GABAergic synaptic transmission, predicting decreased cortical circuit excitability (29, 30). By contrast, increasing *Ube3a* gene dosage reduced circuit excitability by reducing glutamatergic synaptic transmission. These distinct circuit defects are consistent with the notion that different therapeutic targets may be necessary to treat subtypes of ASD.

Ube3a is an E3 ubiquitin ligase, a class of protein that provides substrate specificity to the ubiquitin protein degradation system. Many tens of targets of Ube3a have been identified in cell culture systems (54, 55), in *Drosophila* (56, 57), and recently in mouse brain (19, 20). Our initial screen of potential Ube3a targets only revealed changes in Arc. The pre- and postsynaptic functional defects in glutamate synapses produced by excess Ube3a suggest that several distinct unidentified ubiquitination targets could be regulating excitatory synapse function. Recent studies also indicate that ubiquitination, rather than promoting proteasome degradation, can instead sometimes increase protein stability or alter protein trafficking (58, 59). Alternatively, ubiquitin ligase activity may not be critical to the effects of excess Ube3a on behavior and neuronal circuit function because the protein can also act as steroid hormone transcriptional coactivator independent of its E3 ligase activity (60, 61).

The potential important effects of Ube3a on gene expression are supported by its strong nuclear localization.

The translational value of this new mouse model of ASD lies in its construct and face validity, because it adds excess copies of one gene found within a common CNV region found in nonsyndromic ASD and displays correlates of three core ASD behavioral traits. The predictive validity of this model has not yet been tested due to the lack of drug treatments for the human condition. Current therapies for ASD largely target the comorbid neurologic (epilepsy) and neuropsychiatric (anxiety) conditions. The quantitative measures of social behavior and communication disrupted in this murine model of ASD can serve as a valuable system for preclinical testing of candidate drugs. Further, the detailed mechanistic analysis of neuronal circuit defects made possible by such mouse models of ASD will provide a strong foundation for the rational design of therapeutics aimed at bolstering specific defects in circuit function.

MATERIALS AND METHODS

Generation of mice

Using BAC recombineering techniques, we inserted a 162-kb segment of mouse chromosome 7, containing the entire 78-kb exon-intron coding sequence of Ube3a as well as its 63-kb 5′ and 21-kb 3′ sequences, into FVB embryos to generate transgenic mice (fig. S1). A 3×FLAG tag followed by two stop codons was inserted in-frame after exon 12 to generate two independent founder mice. Transgenic founder offspring were then crossed to produce *Ube3a* 1× or 2× transgenic mice. Genotyping was accomplished by semiquantitative PCR of sequences flanking the FLAG-tagged Ube3a gene with the native gene as an internal control. Primers and detailed protocols are available in the Supplementary Materials and Methods.

Ube3a protein overexpression and function

Ube3a expression was confirmed by Western blot of cortical lysates with both anti-FLAG M2 antibody (Sigma) and anti-Ube3a (BD Biosciences). The ubiquitin ligase activity of Ube3a was assayed by an in vitro target protein degradation assay. Ube3a was immunoprecipitated with anti-FLAG M2 antibodies and protein G magnetic beads (NEB) and eluted in nondenaturing conditions with a 3× FLAG peptide (Sigma). Recombinant Arc (1 μg) (BD Biosciences) was added to 10 μl of immunoprecipitated Ube3a in the presence of 50 ng of E1 and 100 ng of UbcH7 enzymes and 4 μg of hemagglutinin-ubiquitin (Boston BioProducts) (19). Western blots were probed with anti-Arc (Santa Cruz) and quantified with ImageJ (National Institutes of Health). Detailed protocols are available in the Supplementary Materials and Methods.

Three-chamber social interaction testing

Separate cohorts of mice were tested in the three-chamber social test as either juveniles (3 to 4 weeks) or adults (8 to 12 weeks) following previously published protocols (24, 25). For the juvenile test, after a 10-min acclimation period in an empty chamber, a stranger wild-type mouse was placed in a small enclosure in one of the outer chambers, and an empty enclosure was placed in the opposite side. The round wire enclosure (a pencil holder, Office Depot) allowed visual, olfactory, and tactile interaction. The test session lasted 10 min. For the adult test, the enclosures were present during the acclimation, and sessions lasted 5 min. Therefore, in the juvenile test, the comparison was between a novel mouse and a novel object (the enclosure), whereas the adult test compared a novel mouse with a familiar container. To control for novel object preference in the adult, we repeated the test but placed

a novel object (a striped plastic cup) into one of the two enclosures a week after the initial test.

Grooming

Mice were placed in a clean cage in a fume hood in their home room and were allowed to acclimate for 10 min. Mice were then video-recorded for 10 min, and the time spent grooming was measured by an experienced observer (29).

Vocalizations

For urine-induced vocalizations, male mice were single-housed for several days and then exposed to brief (5 min) social interactions with both male and female mice for 4 days before the test. On the fifth day, mice were placed in a small plastic box inside a larger soundproof container. A cotton swab dipped in freshly collected urine pooled from at least 10 females from at least five different cages was suspended from the top of the smaller box, so that the tip was about 5 cm above the floor. An ultrasonic microphone recorded vocalizations and fed data into a computer running Avisoft-Recorder (Avisoft Bioacoustics), which automatically counted the vocalizations over the 5-min test period. For social vocalizations, sex-, age-, and genotype-matched, nonlittermate mice that had never encountered each other before were placed in a small plastic enclosure simultaneously (to avoid resident-intruder aggression), and the number of vocalizations and time spent vocalizing were recorded automatically (UltraVox, Noldus) for 5 min.

Electrophysiology

EPSCs were recorded in voltage-clamp mode with cesium-based artificial intracellular fluid and regular artificial cerebrospinal fluid (ACSF). A bipolar platinum/iridium-stimulating electrode (CE2C55, FHC Inc.) was placed at layer 2/3 of the barrel cortex 200 μm away from the recording site. A glass pipette filled with 0.5 mM bicuculline meth-iodide in ACSF that locally inhibited GABAergic transmission was placed above the soma of the cell being recorded. IPSCs were recorded at a holding potential of +10 mV in the presence of bath 10 μM DNQX (6,7-dinitroquinoxaline-2,3-dione) and 50 μM APV [(2*R*)-amino-5-phosphonopentanoate]. mEPSCs and mIPSCs were recorded at −60 or −80 mV and +10 mV, respectively. Detailed protocols are available in the Supplementary Materials and Methods.

Glutamate iontophoresis—Pyramidal neurons were voltage-clamped at −70 or +40 mV in the presence of 1 μM tetrodotoxin and 100 μM picrotoxin. Iontophoretically applied glutamate (10 mM sodium glutamate in 10 mM Hepes, pH 7.4) was delivered through glass pipettes (4 to 6 megohms when filled with normal internal solution) placed 1 to 2 μm away from the main apical shaft (~15 to 20 μm from cell body).

Minimal stimulation and estimation of vesicle glutamate content—The vesicle glutamate content was estimated by the relative inhibition of mean single fiber EPSC amplitude by the fast off-rate, non-NMDA receptor blocker γ-DGG (300 μM). The higher the percentage inhibition by γ-DGG, the lower the concentration of synaptic glutamate. Detailed protocols are available in the Supplementary Materials and Methods.

Statistical analyses

For behavior analysis, comparisons between two groups used two-tailed unpaired Student's *t* test. Comparisons among multiple groups used one-way analysis of variance (ANOVA) with Dunnett's post hoc test comparing each genotype to wild type; nonsignificant comparisons are not stated in the manuscript. Comparisons involving multiple independent

variables used two-way ANOVAs. Nonnormal data (social vocalizations) were tested with the Kruskal-Wallis test followed by Dunn's multiple comparison post hoc test comparing each genotype to wild type. For electrophysiological data, two-tailed unpaired Student's *t* test was used to compare group means. Kolmogorov-Smirnov test was used to compare cumulative distributions. Mantel-Haenszel χ^2 test was used to compare the ES coupling data. Unbalanced two-way ANOVA was used to compare group variance. Tukey's honestly significant difference test was used to perform post-ANOVA pairwise comparisons. *n* is the number of mice analyzed (behavior and synapse counting), number of pairs of mice analyzed (social vocalizations), or number of cells analyzed (electrophysiology). All data are presented as means ± SEM. $P < 0.05$ was considered statistically significant.

Supplementary Material

Refer to Web version on PubMed Central for supplementary material.

Acknowledgments

We thank X. Wang and O. DiStefano for technical assistance, D. Brown for electron microscopy technical assistance, J. N. Crawley for information on FVB mouse vocalizations, M. W. Anderson for comments on the manuscript, and E. Maratos-Flier for providing behavioral equipment and advice.

Funding: This work was supported in part by the U.S. National Institute of Neurological Disorders and Stroke grants R21NS070295, R01 NS057444, and K02 NS054674-03 (M.P.A.); Nancy Lurie Marks Family Foundation (M.P.A.); Autism Speaks/U.S. National Alliance for Autism Research (M.P.A.); U.S. National Institute of Mental Health National Research Service Award Fellowship F32 MH087085 (S.E.P.S.); and Beth Israel Deaconess Medical Center.

REFERENCES AND NOTES

1. Levy SE, Mandell DS, Schultz RT. Autism. Lancet. 2009; 374:1627–1638. [PubMed: 19819542]
2. Abrahams BS, Geschwind DH. Advances in autism genetics: On the threshold of a new neurobiology. Nat Rev Genet. 2008; 9:341–355. [PubMed: 18414403]
3. Glessner JT, Wang K, Cai G, Korvatska O, Kim CE, Wood S, Zhang H, Estes A, Brune CW, Bradfield JP, Imielinski M, Frackelton EC, Reichert J, Crawford EL, Munson J, Sleiman PM, Chiavacci R, Annaiah K, Thomas K, Hou C, Glaberson W, Flory J, Otieno F, Garris M, Soorya L, Klei L, Piven J, Meyer KJ, Anagnostou E, Sakurai T, Game RM, Rudd DS, Zurawiecki D, McDougle CJ, Davis LK, Miller J, Posey DJ, Michaels S, Kolevzon A, Silverman JM, Bernier R, Levy SE, Schultz RT, Dawson G, Owley T, McMahon WM, Wassink TH, Sweeney JA, Nurnberger JI, Coon H, Sutcliffe JS, Minshew NJ, Grant SF, Bucan M, Cook EH, Buxbaum JD, Devlin B, Schellenberg GD, Hakonarson H. Autism genome-wide copy number variation reveals ubiquitin and neuronal genes. Nature. 2009; 459:569–573. [PubMed: 19404257]
4. Morrow EM, Yoo SY, Flavell SW, Kim TK, Lin Y, Hill RS, Mukaddes NM, Balkhy S, Gascon G, Hashmi A, Al-Saad S, Ware J, Joseph RM, Greenblatt R, Gleason D, Ertelt JA, Apse KA, Bodell A, Partlow JN, Barry B, Yao H, Markianos K, Ferland RJ, Greenberg ME, Walsh CA. Identifying autism loci and genes by tracing recent shared ancestry. Science. 2008; 321:218–223. [PubMed: 18621663]
5. Pinto D, Pagnamenta AT, Klei L, Anney R, Merico D, Regan R, Conroy J, Magalhaes TR, Correia C, Abrahams BS, Almeida J, Bacchelli E, Bader GD, Bailey AJ, Baird G, Battaglia A, Berney T, Bolshakova N, Bölte S, Bolton PF, Bourgeron T, Brennan S, Brian J, Bryson SE, Carson AR, Casallo G, Casey J, Chung BH, Cochrane L, Corsello C, Crawford EL, Crossett A, Cytrynbaum C, Dawson G, de Jonge M, Delorme R, Drmic I, Duketis E, Duque F, Estes A, Farrar P, Fernandez BA, Folstein SE, Fombonne E, Freitag CM, Gilbert J, Gillberg C, Glessner JT, Goldberg J, Green A, Green J, Guter SJ, Hakonarson H, Heron EA, Hill M, Holt R, Howe JL, Hughes G, Hus V, Igliozzi R, Kim C, Klauck SM, Kolevzon A, Korvatska O, Kustanovich V, Lajonchere CM, Lamb JA, Laskawiec M, Leboyer M, Le Couteur A, Leventhal BL, Lionel AC, Liu XQ, Lord C, Lotspeich L, Lund SC, Maestrini E, Mahoney W, Mantoulan C, Marshall CR, McConachie H, McDougle CJ,

McGrath J, McMahon WM, Merikangas A, Migita O, Minshew NJ, Mirza GK, Munson J, Nelson SF, Noakes C, Noor A, Nygren G, Oliveira G, Papanikolaou K, Parr JR, Parrini B, Paton T, Pickles A, Pilorge M, Piven J, Ponting CP, Posey DJ, Poustka A, Poustka F, Prasad A, Ragoussis J, Renshaw K, Rickaby J, Roberts W, Roeder K, Roge B, Rutter ML, Bierut LJ, Rice JP, Salt J, Sansom K, Sato D, Segurado R, Sequeira AF, Senman L, Shah N, Sheffield VC, Soorya L, Sousa I, Stein O, Sykes N, Stoppioni V, Strawbridge C, Tancredi R, Tansey K, Thiruvahindrapduram B, Thompson AP, Thomson S, Tryfon A, Tsiantis J, Van Engeland H, Vincent JB, Volkmar F, Wallace S, Wang K, Wang Z, Wassink TH, Webber C, Weksberg R, Wing K, Wittemeyer K, Wood S, Wu J, Yaspan BL, Zurawiecki D, Zwaigenbaum L, Buxbaum JD, Cantor RM, Cook EH, Coon H, Cuccaro ML, Devlin B, Ennis S, Gallagher L, Geschwind DH, Gill M, Haines JL, Hallmayer J, Miller J, Monaco AP, Nurnberger JI Jr, Paterson AD, Pericak-Vance MA, Schellenberg GD, Szatmari P, Vicente AM, Vieland VJ, Wijsman EM, Scherer SW, Sutcliffe JS, Betancur C. Functional impact of global rare copy number variation in autism spectrum disorders. Nature. 2010; 466:368–372. [PubMed: 20531469]

6. Sebat J, Lakshmi B, Malhotra D, Troge J, Lese-Martin C, Walsh T, Yamrom B, Yoon S, Krasnitz A, Kendall J, Leotta A, Pai D, Zhang R, Lee YH, Hicks J, Spence SJ, Lee AT, Puura K, Lehtimäki T, Ledbetter D, Gregersen PK, Bregman J, Sutcliffe JS, Jobanputra V, Chung W, Warburton D, King MC, Skuse D, Geschwind DH, Gilliam TC, Ye K, Wigler M. Strong association of de novo copy number mutations with autism. Science. 2007; 316:445–449. [PubMed: 17363630]
7. Weiss LA, Shen Y, Korn JM, Arking DE, Miller DT, Fossdal R, Saemundsen E, Stefansson H, Ferreira MA, Green T, Platt OS, Ruderfer DM, Walsh CA, Altshuler D, Chakravarti A, Tanzi RE, Stefansson K, Santangelo SL, Gusella JF, Sklar P, Wu BL, Daly MJ. Autism Consortium. Association between microdeletion and microduplication at 16p11.2 and autism. N Engl J Med. 2008; 358:667–675. [PubMed: 18184952]
8. Hogart A, Wu D, LaSalle JM, Schanen NC. The comorbidity of autism with the genomic disorders of chromosome 15q11.2–q13. Neurobiol Dis. 2010; 38:181–191. [PubMed: 18840528]
9. Albrecht U, Sutcliffe JS, Cattanach BM, Beechey CV, Armstrong D, Eichele G, Beaudet AL. Imprinted expression of the murine Angelman syndrome gene, *Ube3a*, in hippocampal and Purkinje neurons. Nat Genet. 1997; 17:75–78. [PubMed: 9288101]
10. Jiang YH, Armstrong D, Albrecht U, Atkins CM, Noebels JL, Eichele G, Sweatt JD, Beaudet AL. Mutation of the Angelman ubiquitin ligase in mice causes increased cytoplasmic p53 and deficits of contextual learning and long-term potentiation. Neuron. 1998; 21:799–811. [PubMed: 9808466]
11. Kishino T, Lalande M, Wagstaff J. UBE3A/E6-AP mutations cause Angelman syndrome. Nat Genet. 1997; 15:70–73. [PubMed: 8988171]
12. Dindot SV, Antalffy BA, Bhattacharjee MB, Beaudet AL. The Angelman syndrome ubiquitin ligase localizes to the synapse and nucleus, and maternal deficiency results in abnormal dendritic spine morphology. Hum Mol Genet. 2008; 17:111–118. [PubMed: 17940072]
13. Jiang YH, Pan Y, Zhu L, Landa L, Yoo J, Spencer C, Lorenzo I, Brilliant M, Noebels J, Beaudet AL. Altered ultrasonic vocalization and impaired learning and memory in Angelman syndrome mouse model with a large maternal deletion from *Ube3a* to *Gabrb3*. PLoS One. 2010; 5:e12278. [PubMed: 20808828]
14. Weeber EJ, Jiang YH, Elgersma Y, Varga AW, Carrasquillo Y, Brown SE, Christian JM, Mirnikjoo B, Silva A, Beaudet AL, Sweatt JD. Derangements of hippocampal calcium/calmodulin-dependent protein kinase II in a mouse model for Angelman mental retardation syndrome. J Neurosci. 2003; 23:2634–2644. [PubMed: 12684449]
15. van Woerden GM, Harris KD, Hojjati MR, Gustin RM, Qiu S, de Avila Freire R, Jiang YH, Elgersma Y, Weeber EJ. Rescue of neurological deficits in a mouse model for Angelman syndrome by reduction of αCaMKII inhibitory phosphorylation. Nat Neurosci. 2007; 10:280–282. [PubMed: 17259980]
16. Sato M, Stryker MP. Genomic imprinting of experience-dependent cortical plasticity by the ubiquitin ligase gene *Ube3a*. Proc Natl Acad Sci USA. 2010; 107:5611–5616. [PubMed: 20212164]
17. Yashiro K, Riday TT, Condon KH, Roberts AC, Bernardo DR, Prakash R, Weinberg RJ, Ehlers MD, Philpot BD. Ube3a is required for experience-dependent maturation of the neocortex. Nat Neurosci. 2009; 12:777–783. [PubMed: 19430469]

18. Scheffner M, Huibregtse JM, Vierstra RD, Howley PM. The HPV-16 E6 and E6-AP complex functions as a ubiquitin-protein ligase in the ubiquitination of p53. Cell. 1993; 75:495–505. [PubMed: 8221889]
19. Greer PL, Hanayama R, Bloodgood BL, Mardinly AR, Lipton DM, Flavell SW, Kim TK, Griffith EC, Waldon Z, Maehr R, Ploegh HL, Chowdhury S, Worley PF, Steen J, Greenberg ME. The Angelman syndrome protein Ube3A regulates synapse development by ubiquitinating Arc. Cell. 2010; 140:704–716. [PubMed: 20211139]
20. Margolis SS, Salogiannis J, Lipton DM, Mandel-Brehm C, Wills ZP, Mardinly AR, Hu L, Greer PL, Bikoff JB, Ho HY, Soskis MJ, Sahin M, Greenberg ME. EphB-mediated degradation of the RhoA GEF Ephexin5 relieves a developmental brake on excitatory synapse formation. Cell. 2010; 143:442–455. [PubMed: 21029865]
21. Zhou YD, Lee S, Jin Z, Wright M, Smith SE, Anderson MP. Arrested maturation of excitatory synapses in autosomal dominant lateral temporal lobe epilepsy. Nat Med. 2009; 15:1208–1214. [PubMed: 19701204]
22. Landers M, Bancescu DL, Le Meur E, Rougeulle C, Glatt-Deeley H, Brannan C, Muscatelli F, Lalande M. Regulation of the large (~1000 kb) imprinted murine *Ube3a* antisense transcript by alternative exons upstream of *Snurf*/*Snrpn*. Nucleic Acids Res. 2004; 32:3480–3492. [PubMed: 15226413]
23. Gustin RM, Bichell TJ, Bubser M, Daily J, Filonova I, Mrelashvili D, Deutch AY, Colbran RJ, Weeber EJ, Haas KF. Tissue-specific variation of Ube3a protein expression in rodents and in a mouse model of Angelman syndrome. Neurobiol Dis. 2010; 39:283–291. [PubMed: 20423730]
24. Crawley JN. Mouse behavioral assays relevant to the symptoms of autism. Brain Pathol. 2007; 17:448–459. [PubMed: 17919130]
25. Smith SE, Li J, Garbett K, Mirnics K, Patterson PH. Maternal immune activation alters fetal brain development through interleukin-6. J Neurosci. 2007; 27:10695–10702. [PubMed: 17913903]
26. Holy TE, Guo Z. Ultrasonic songs of male mice. PLoS Biol. 2005; 3:e386. [PubMed: 16248680]
27. Ehret G. Infant rodent ultrasounds—A gate to the understanding of sound communication. Behav Genet. 2005; 35:19–29. [PubMed: 15674530]
28. Blundell J, Blaiss CA, Etherton MR, Espinosa F, Tabuchi K, Walz C, Bolliger MF, Südhof TC, Powell CM. Neuroligin-1 deletion results in impaired spatial memory and increased repetitive behavior. J Neurosci. 2010; 30:2115–2129. [PubMed: 20147539]
29. Etherton MR, Blaiss CA, Powell CM, Sudhof TC. Mouse neurexin-1α deletion causes correlated electrophysiological and behavioral changes consistent with cognitive impairments. Proc Natl Acad Sci USA. 2009; 106:17998–18003. [PubMed: 19822762]
30. Tabuchi K, Blundell J, Etherton MR, Hammer RE, Liu X, Powell CM, Sudhof TC. A neuroligin-3 mutation implicated in autism increases inhibitory synaptic transmission in mice. Science. 2007; 318:71–76. [PubMed: 17823315]
31. Chao HT, Chen H, Samaco RC, Xue M, Chahrour M, Yoo J, Neul JL, Gong S, Lu HC, Heintz N, Ekker M, Rubenstein JL, Noebels JL, Rosenmund C, Zoghbi HY. Dysfunction in GABA signalling mediates autism-like stereotypies and Rett syndrome phenotypes. Nature. 2010; 468:263–269. [PubMed: 21068835]
32. Liu G, Choi S, Tsien RW. Variability of neurotransmitter concentration and nonsaturation of postsynaptic AMPA receptors at synapses in hippocampal cultures and slices. Neuron. 1999; 22:395–409. [PubMed: 10069344]
33. Chadman KK, Gong S, Scattoni ML, Boltuck SE, Gandhy SU, Heintz N, Crawley JN. Minimal aberrant behavioral phenotypes of neuroligin-3 R451C knockin mice. Autism Res. 2008; 1:147–158. [PubMed: 19360662]
34. Bangash MA, Park JM, Melnikova T, Wang D, Jeon SK, Lee D, Syeda S, Kim J, Kouser M, Schwartz J, Cui Y, Zhao X, Speed HE, Kee SE, Tu JC, Hu JH, Petralia RS, Linden DJ, Powell CM, Savonenko A, Xiao B, Worley PF. Enhanced polyubiquitination of Shank3 and NMDA receptor in a mouse model of autism. Cell. 2011; 145:758–772. [PubMed: 21565394]
35. Wang X, McCoy PA, Rodriguiz RM, Pan Y, Je HS, Roberts AC, Kim CJ, Berrios J, Colvin JS, Bousquet-Moore D, Lorenzo I, Wu G, Weinberg RJ, Ehlers MD, Philpot BD, Beaudet AL, Wetsel

WC, Jiang YH. Synaptic dysfunction and abnormal behaviors in mice lacking major isoforms of *Shank3*. Hum Mol Genet. 2011; 20:3093–3108. [PubMed: 21558424]

36. Peça J, Feliciano C, Ting JT, Wang W, Wells MF, Venkatraman TN, Lascola CD, Fu Z, Feng G. Shank3 mutant mice display autistic-like behaviours and striatal dysfunction. Nature. 2011; 472:437–442. [PubMed: 21423165]
37. Bozdagi O, Sakurai T, Papapetrou D, Wang X, Dickstein DL, Takahashi N, Kajiwara Y, Yang M, Katz AM, Scattoni ML, Harris MJ, Saxena R, Silverman JL, Crawley JN, Zhou Q, Hof PR, Buxbaum JD. Haploinsufficiency of the autism-associated Shank3 gene leads to deficits in synaptic function, social interaction, and social communication. Mol Autism. 2010; 1:15. [PubMed: 21167025]
38. Bakker CE, Verheij C, Willemsen R, van der Helm R, Oerlemans F, Vermey M, Bygrave A, Hoogeveen AT, Oostra BA, Reyniers E, De Boule K, D'Hooge R, Cras P, van Velzen D, Nagels G, Martin J-J, De Deyn PP, Darby JK, Willems PJ. The Dutch-Belgian Fragile X Consorthium. *Fmr1* knockout mice: A model to study fragile X mental retardation. Cell. 1994; 78:23–33. [PubMed: 8033209]
39. Shahbazian M, Young J, Yuva-Paylor L, Spencer C, Antalffy B, Noebels J, Armstrong D, Paylor R, Zoghbi H. Mice with truncated MeCP2 recapitulate many Rett syndrome features and display hyperacetylation of histone H3. Neuron. 2002; 35:243–254. [PubMed: 12160743]
40. McFarlane HG, Kusek GK, Yang M, Phoenix JL, Bolivar VJ, Crawley JN. Autism-like behavioral phenotypes in BTBR T+tf/J mice. Genes Brain Behav. 2008; 7:152–163. [PubMed: 17559418]
41. Hamilton SM, Spencer CM, Harrison WR, Yuva-Paylor LA, Graham DF, Daza RA, Hevner RF, Overbeek PA, Paylor R. Multiple autism-like behaviors in a novel trans-genic mouse model. Behav Brain Res. 2011; 218:29–41. [PubMed: 21093492]
42. Shi L, Fatemi SH, Sidwell RW, Patterson PH. Maternal influenza infection causes marked behavioral and pharmacological changes in the offspring. J Neurosci. 2003; 23:297–302. [PubMed: 12514227]
43. Dennis NR, Veltman MW, Thompson R, Craig E, Bolton PF, Thomas NS. Clinical findings in 33 subjects with large supernumerary marker(15) chromosomes and 3 subjects with triplication of 15q11-q13. Am J Med Genet A. 2006; 140:434–441. [PubMed: 16470730]
44. Baron CA, Tepper CG, Liu SY, Davis RR, Wang NJ, Schanen NC, Gregg JP. Genomic and functional profiling of duplicated chromosome 15 cell lines reveal regulatory alterations in UBE3A-associated ubiquitin–proteasome pathway processes. Hum Mol Genet. 2006; 15:853–869. [PubMed: 16446308]
45. Hogart A, Leung KN, Wang NJ, Wu DJ, Driscoll J, Vallero RO, Schanen NC, LaSalle JM. Chromosome 15q11–13 duplication syndrome brain reveals epigenetic alterations in gene expression not predicted from copy number. J Med Genet. 2009; 46:86–93. [PubMed: 18835857]
46. Nakatani J, Tamada K, Hatanaka F, Ise S, Ohta H, Inoue K, Tomonaga S, Watanabe Y, Chung YJ, Banerjee R, Iwamoto K, Kato T, Okazawa M, Yamauchi K, Tanda K, Takao K, Miyakawa T, Bradley A, Takumi T. Abnormal behavior in a chromosome-engineered mouse model for human 15q11-13 duplication seen in autism. Cell. 2009; 137:1235–1246. [PubMed: 19563756]
47. Kashiwagi A, Meguro M, Hoshiya H, Haruta M, Ishino F, Shibahara T, Oshimura M. Predominant maternal expression of the mouse *Atp10c* in hippocampus and olfactory bulb. J Hum Genet. 2003; 48:194–198. [PubMed: 12730723]
48. Meguro M, Kashiwagi A, Mitsuya K, Nakao M, Kondo I, Saitoh S, Oshimura M. A novel maternally expressed gene, *ATP10C*, encodes a putative aminophospholipid translocase associated with Angelman syndrome. Nat Genet. 2001; 28:19–20. [PubMed: 11326269]
49. Kayashima T, Yamasaki K, Joh K, Yamada T, Ohta T, Yoshiura K, Matsumoto N, Nakane Y, Mukai T, Niikawa N, Kishino T. *Atp10a*, the mouse ortholog of the human imprinted *ATP10A* gene, escapes genomic imprinting. Genomics. 2003; 81:644–647. [PubMed: 12782135]
50. Nishimura Y, Martin CL, Vazquez-Lopez A, Spence SJ, Alvarez-Retuerto AI, Sigman M, Steindler C, Pellegrini S, Schanen NC, Warren ST, Geschwind DH. Genome-wide expression profiling of lymphoblastoid cell lines distinguishes different forms of autism and reveals shared pathways. Hum Mol Genet. 2007; 16:1682–1698. [PubMed: 17519220]

51. Hogart A, Nagarajan RP, Patzel KA, Yasui DH, Lasalle JM. 15q11-13 $GABA_A$ receptor genes are normally biallelically expressed in brain yet are subject to epigenetic dysregulation in autism-spectrum disorders. Hum Mol Genet. 2007; 16:691–703. [PubMed: 17339270]
52. Shepherd JD, Rumbaugh G, Wu J, Chowdhury S, Plath N, Kuhl D, Huganir RL, Worley PF. Arc/Arg3.1 mediates homeostatic synaptic scaling of AMPA receptors. Neuron. 2006; 52:475–484. [PubMed: 17088213]
53. Miura K, Kishino T, Li E, Webber H, Dikkes P, Holmes GL, Wagstaff J. Neurobehavioral and electroencephalographic abnormalities in *Ube3a* maternal-deficient mice. Neurobiol Dis. 2002; 9:149–159. [PubMed: 11895368]
54. Mishra A, Jana NR. Regulation of turnover of tumor suppressor p53 and cell growth by E6-AP, a ubiquitin protein ligase mutated in Angelman mental retardation syndrome. Cell Mol Life Sci. 2008; 65:656–666. [PubMed: 18193166]
55. Mulherkar SA, Sharma J, Jana NR. The ubiquitin ligase E6-AP promotes degradation of α-synuclein. J Neurochem. 2009; 110:1955–1964. [PubMed: 19645749]
56. Ferdousy F, Bodeen W, Summers K, Doherty O, Wright O, Elsisi N, Hilliard G, O'Donnell JM, Reiter LT. *Drosophila* Ube3a regulates monoamine synthesis by increasing GTP cyclo-hydrolase I activity via a non-ubiquitin ligase mechanism. Neurobiol Dis. 2011; 41:669–677. [PubMed: 21147225]
57. Reiter LT, Seagroves TN, Bowers M, Bier E. Expression of the Rho-GEF Pbl/ECT2 is regulated by the UBE3A E3 ubiquitin ligase. Hum Mol Genet. 2006; 15:2825–2835. [PubMed: 16905559]
58. Hicke L, Dunn R. Regulation of membrane protein transport by ubiquitin and ubiquitin-binding proteins. Annu Rev Cell Dev Biol. 2003; 19:141–172. [PubMed: 14570567]
59. Mukhopadhyay D, Riezman H. Proteasome-independent functions of ubiquitin in endocytosis and signaling. Science. 2007; 315:201–205. [PubMed: 17218518]
60. Nawaz Z, Lonard DM, Smith CL, Lev-Lehman E, Tsai SY, Tsai MJ, O'Malley BW. The Angelman syndrome-associated protein, E6-AP, is a coactivator for the nuclear hormone receptor superfamily. Mol Cell Biol. 1999; 19:1182–1189. [PubMed: 9891052]
61. Ramamoorthy S, Nawaz Z. E6-associated protein (E6-AP) is a dual function coactivator of steroid hormone receptors. Nucl Recept Signal. 2008; 6:e006. [PubMed: 18432313]

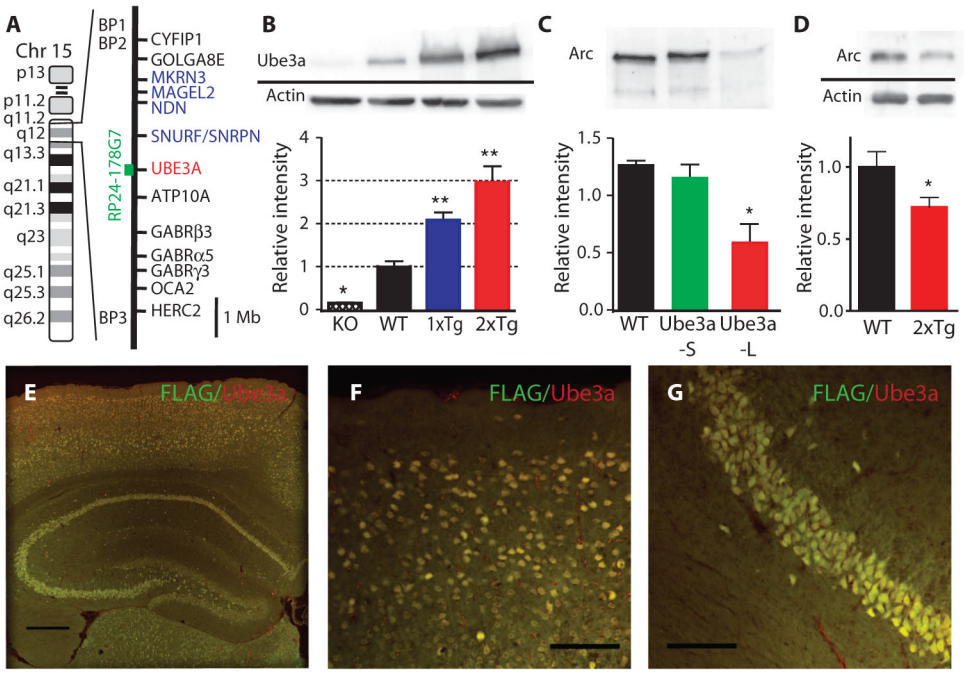

Fig. 1.

Expression of functional, full-length *Ube3a* gene BAC transgene Ube3a protein in the native expression pattern. (**A**) Schematic representation of the human genes located between breakpoint (BP) 1 and BP3 in the 15q11-13 region. Paternally expressed genes are blue, maternally expressed genes are red, and the location of the genomic DNA contained in the BAC is green. (**B**) Quantification of Ube3a protein in maternal Ube3a knockout (KO), wild-type (WT), 1×Tg, and 2×Tg *Ube3a* transgenic mice (total brain protein, Ube3a antibody) (ANOVA: $F_{(3,24)} = 26.95$; $^{*}P < 0.05$; $^{**}P < 0.001$ by Dunnett's post hoc, $n = 4$ to 11). (**C**) Western blot of Arc assessing degradation in vitro by transgenic Ube3a isoforms 2 and 3 (Ube3a-L) and isoform 1 (Ube3a-S). Ube3a was immunoprecipitated with FLAG antibody from total brain (ANOVA: $F_{(2,6)} = 9.93$; $^{*}P < 0.05$ by Dunnett's post hoc, $n = 3$ independent in vitro assays). (**D**) Western blot of Arc in the barrel cortex in WT and 2×Tg mice. $n = 10$ to 12. $^{*}P = 0.03$, two-tailed, unpaired t test. (**E** to **G**) Double immunofluorescence staining for total Ube3a (red) and Ube3a-FLAG transgene (green) (colocalization is shown in yellow) in (E) hippocampus and cortex, (F) superficial layers of the barrel cortex, and (G) CA3 of the hippocampus. Scale bars, 500 μm (E) and 100 μm [(F) and (G)].

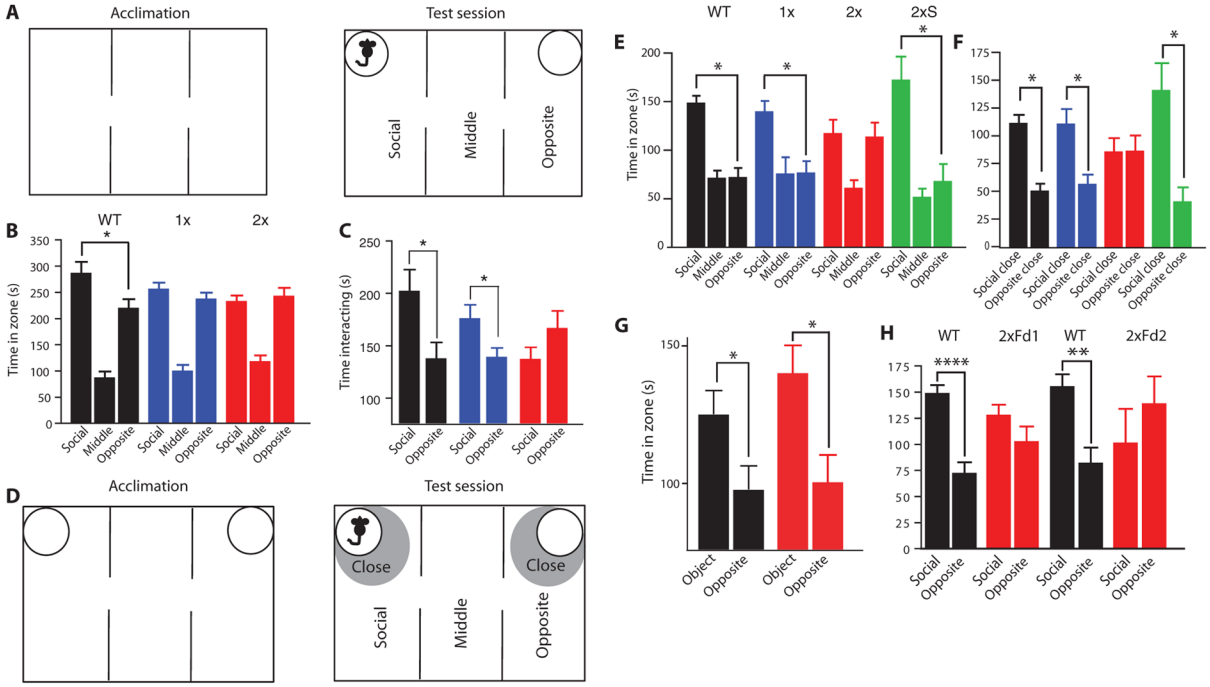

Fig. 2.

Effects of increased *Ube3a* gene dosage on mouse social behavior. (**A**) Diagram of three-chamber social interaction test with acclimation to arena only and choice between a novel container containing a novel mouse and a novel empty container. (**B**) Time in social, middle, or opposite zone in juvenile WT, 1×Tg, and 2×Tg mice (**P* = 0.0162 comparing within-genotype "Social" and "Opposite" by *t* test). (**C**) Time spent interacting with either the caged mouse (social) or the empty cage (opposite). (**P* = 0.0157 and 0.0186, respectively, *t* test). $n_{(WT,\ 1\times,\ 2\times)}$ = 11, 15, and 12. (**D**) Diagram of a modified three-chambered social interaction test with acclimation to arena and cages (left) and a test session (right) in which the mouse chooses between exploring a familiar empty cage or a cage containing a novel mouse. (**E**) Time in social, middle, or opposite zone in adult WT, 1×Tg-L, 2×Tg-L, and 2×Tg-S mice. **P* < 0.002, *t* test. (**F**) Time in area proximal to the enclosures (dark circles, "Close" zone). **P* < 0.005, *t* test. $n_{(WT,\ 1\times,\ 2\times)}$ = 17, 10, and 15. (**G**) Time spent in proximity to a caged object after acclimation to chamber and cages, which tests for novel object exploration. **P* < 0.03, *t* test, comparing within-genotype "Object" and "Opposite"; *n* = 11 to 13. (**H**) Time spent in social and opposite zone for independent *Ube3a* transgenic founder lines 1 (Fd1) and 2 (Fd2) (*n* = 10 and 5) and WT littermates (*n* = 7 and 4). ***P* < 0.01; *****P* < 0.001, *t* test. Color code (used throughout): WT (black), single-transgenic long-form *Ube3a* (1×, blue), double-transgenic long-form *Ube3a* (2×, red), and double-transgenic short-form "inactive" *Ube3a* (2×S, green).

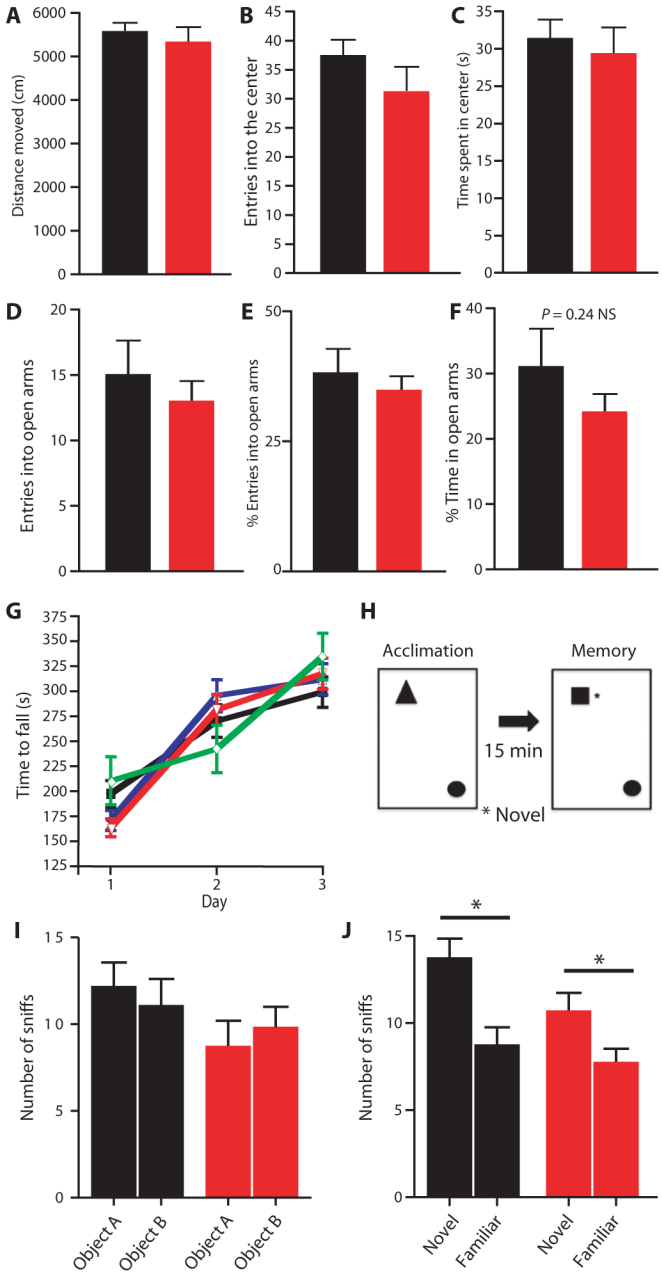

Fig. 3.

Effects of increased *Ube3a* gene dosage on anxiety-like and exploratory behavior, rotorod motor performance, or short-term object memory. (**A** to **C**) The open field tests exploratory behavior, comparing (A) distance traveled, (B) numbers of entries into the center, and (C) time spent in the center of an open field in double-transgenic long-form *Ube3a* (2×, red) and WT littermates. (**D** to **F**) The elevated plus maze tests anxiety-like behavior, assessing (D) number of entries into the open arms, (E) percentage of entries into the open arms, and (F) percent time spent in the open arms (NS, not significant). (**G**) The accelerating rotorod assesses motor performance in mice, comparing time to fall during three sequential days. (**H** to **J**) Short-term memory test in mice is diagrammed (H) and examines (I) number of object exploratory sniffs with first exposure to two novel objects during acclimation phase of

memory test (left) and (J) number of object exploratory sniffs after one object is replaced by a new novel object (right), the memory phase of the test. (*$P < 0.05$, within genotype, *t* test). For complete statistics, see table S1.

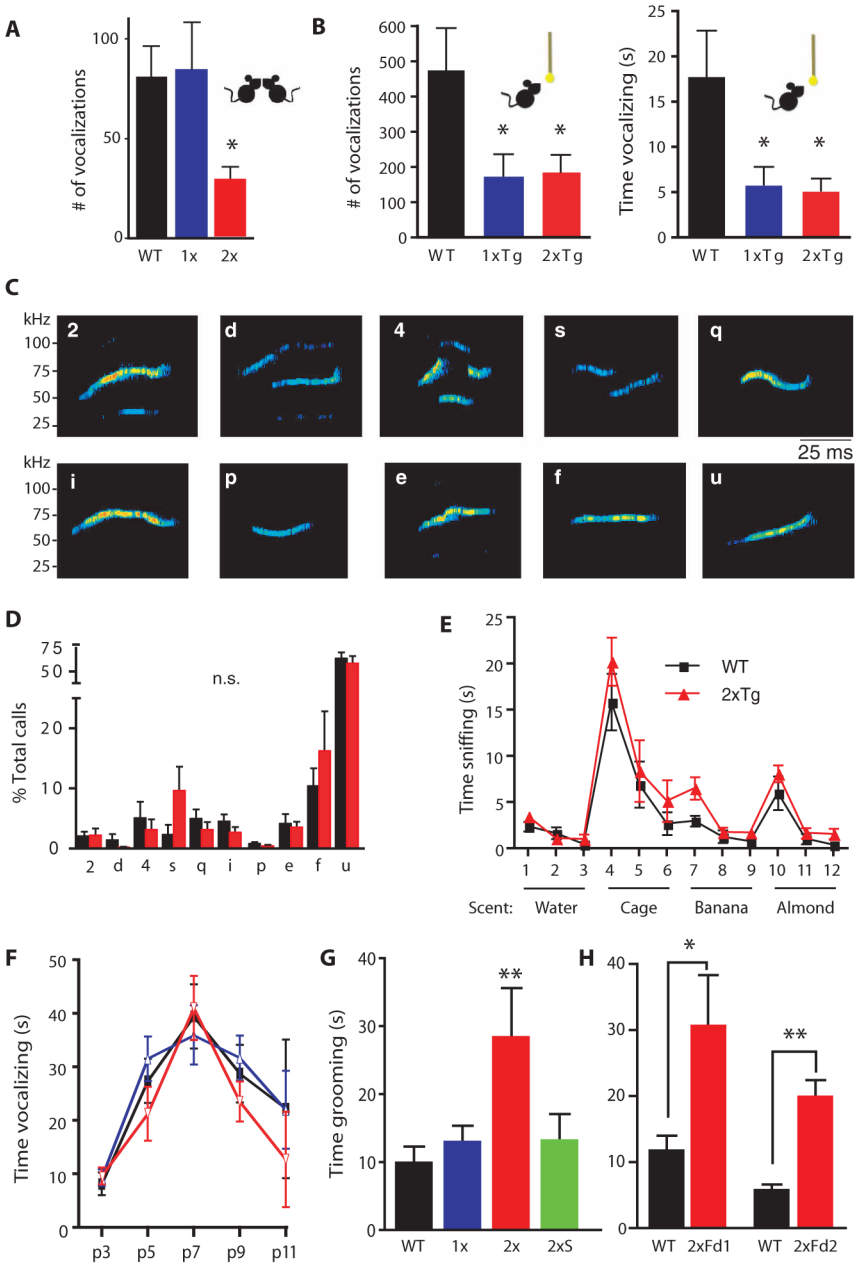

Fig. 4.

Effect of increased *Ube3a* gene dosage on ultrasonic vocalizations and repetitive self-grooming. (**A**) Number of social ultrasonic vocalizations made by pairs of genotype-and sex-matched mice (Kruskal-Wallis test: $H = 7.76$, df = 2, $P = 0.021$, $^*P < 0.05$ by Dunn's multiple comparison post hoc, $n = 8$ to 14 pairs). (**B**) Ultrasonic vocalization responses of male mice to female urine as scored by number (ANOVA: $F_{(2,22)} = 4.52$, $P = 0.023$, $^*P < 0.05$ by Dunnett's post hoc) and time spent vocalizing (ANOVA: $F_{(2,22)} = 5.31$, $P = 0.013$, $^*P < 0.05$ by Dunnett's post hoc). $n = 7$ to 11. (**C** and **D**) Vocalization types, representative examples, and distribution in urine-exposed males, distinguished by shape and harmonics. n.s., not significant by ANOVA. (**E**) Time spent sniffing in the olfactory habituation/dishabituation test (genotype: two-way ANOVA: $F_{(1,132)} = 2.723$, $P = 0.12$, $n = 7$). (**F**)

Ultrasonic vocalizations of pups during acute maternal separation (ANOVA: $F_{(2,262)} = 0.87$, $P = 0.42$, $n = 10$ to 14). (**G**) Repetitive self-grooming (ANOVA: $F_{(2,34)} = 5.41$, $P = 0.0095$, $^{**}P < 0.01$ by Dunnett's post hoc, $n = 11$ to 12). (**H**) Repetitive self-grooming in independent *Ube3a* transgenic founder lines Fd1 ($n_{WT,\ 2\times} = 10$ and 14) and Fd2 ($n_{WT,\ 2\times} =$ 3,5). $^{*}P = 0.01$; $^{**}P = 0.004$, *t* test.

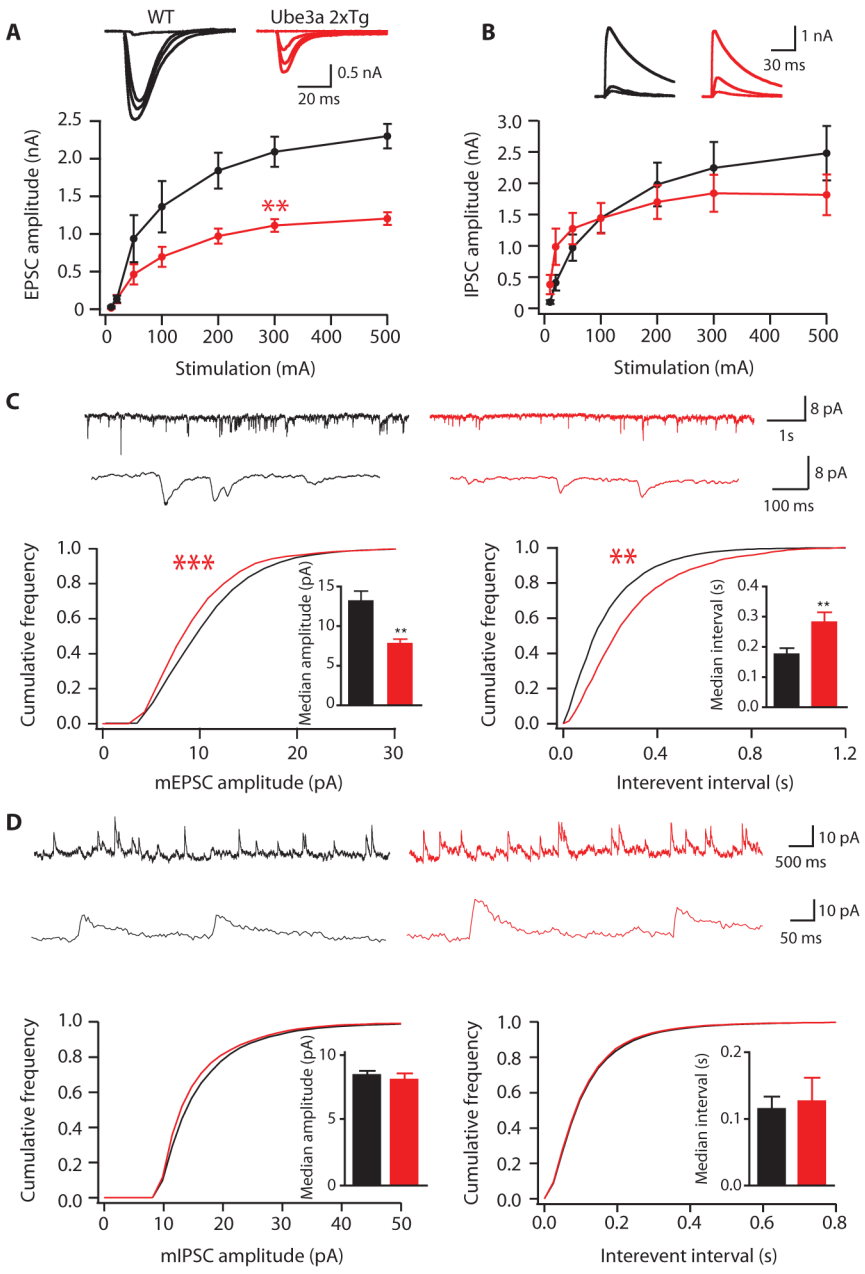

Fig. 5.

Effect of increased (2×Tg) *Ube3a* gene dosage on excitatory and inhibitory synaptic transmission in slices from somatosensory whisker barrel cortex layer 2/3 pyramidal neurons. Black, WT; red, Ube3a 2×Tg. (**A**) Evoked EPSC traces and graph (ANOVA: $F_{(1,97)} = 41.45$, $^{**}P < 0.001$, $n = 6$ to 8). (**B**) Evoked IPSC traces and graph (ANOVA: $F_{(1,83)} = 0.03$, $P = 0.8551$, $n = 6$). (**C**) mEPSC traces (top) and cumulative frequency plots of amplitude (bottom, left) and interevent interval (bottom, right) (Kolmogorov-Smirnov test: $^{**}P < 0.01$, $^{***}P < 0.001$; $n = 9$ to 11). (Insets) Median mEPSC amplitude (left; $P < 0.01$, *t* test) and frequency (right; $P < 0.01$, *t* test; $n = 9$ to 11). (**D**) mIPSC traces and cumulative amplitude (left) and frequency (right) plots ($P > 0.05$, Kolmogorov-Smirnov test; $n = 9$ to

11). (Insets) Median mIPSC amplitude (left) and frequency (right) compared across genotypes ($P > 0.05$, *t* test).

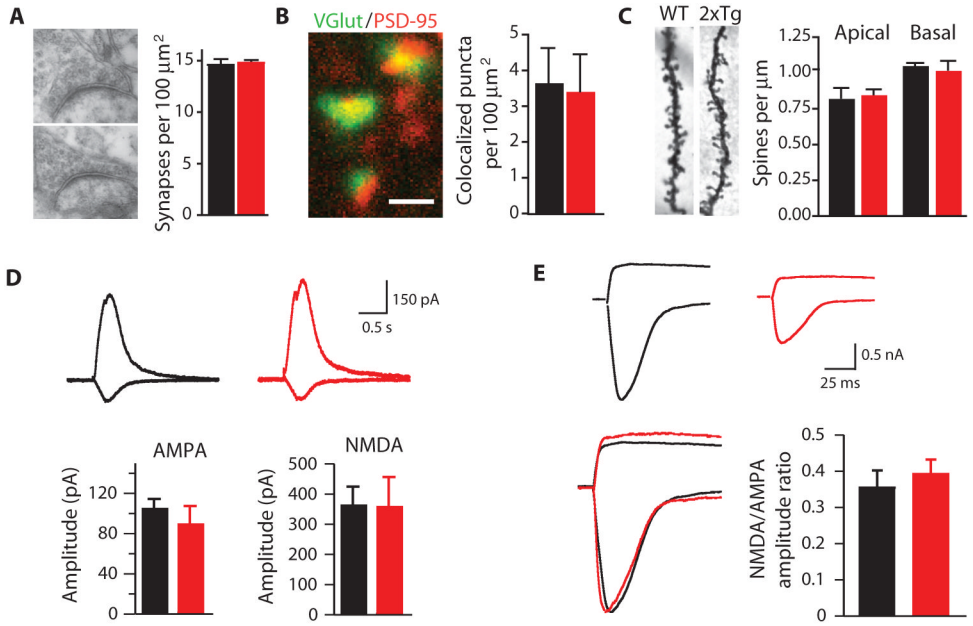

Fig. 6.

Effect of increased (2×Tg) *Ube3a* gene dosage on glutamate synapse number and postsynaptic glutamate receptor currents. Black, WT; red, Ube3a 2×Tg. (**A**) Synapse number, as measured by electron microscopy ($P = 0.67$, *t* test; $n = 3$ animals per group; 28 to 32 micrographs per animal). (**B**) Colocalized immunostaining of presynaptic (VGlut1) and postsynaptic (PSD-95) synaptic markers (scale bar, 1 µm; $P = 0.8706$, *t* test; $n = 4$ animals per group; eight or more micrographs per animal). (**C**) Spine number per dendrite length, as shown by Golgi staining (apical: $P = 0.64$; basal: $P = 0.77$, *t* test; $n = 4$ animals per group; ≥10 dendrites per animal). (**D**) Glutamate ionophoresis–induced AMPA and NMDA currents (AMPA: $P = 0.46$, *t* test; $n = 5$ to 6; NMDA: $P = 0.97$, *t* test; $n = 3$ to 6). (**E**) Fiber stimulation–evoked AMPA/NMDA traces (above, unscaled; below, scaled to WT) and ratio ($P = 0.54$, *t* test; $n = 6$ to 8).

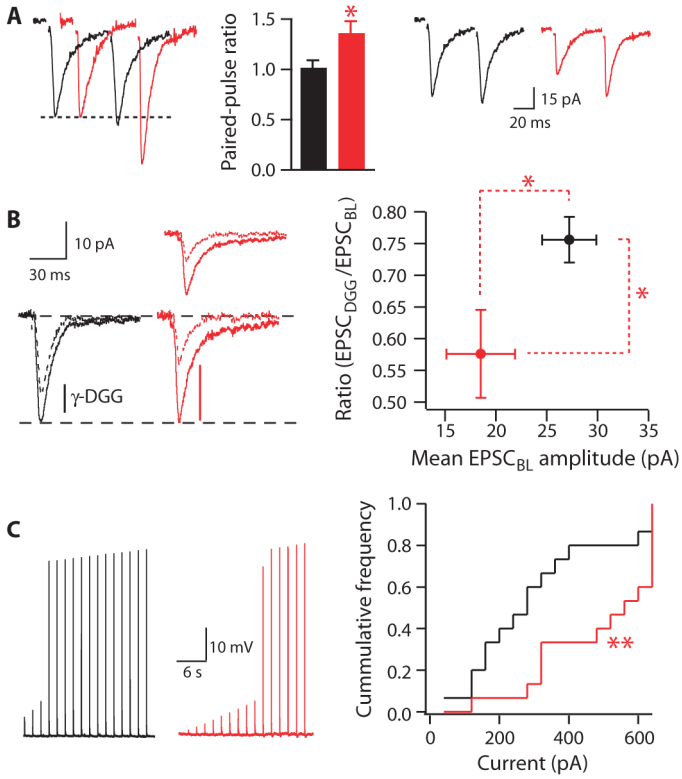

Fig. 7.

Effect of increased (2×Tg) *Ube3a* gene dosage on glutamate synapse release probability, synaptic glutamate concentration, and ES coupling. Black, WT; red, Ube3a 2×Tg. (**A**) Representative unscaled paired-pulse traces (right), traces scaled to match first pulse to WT (left), and bar graph ($P = 0.028$, *t* test; $n = 7$ to 10). (**B**) Representative traces of unscaled (above) and scaled-to-WT (below) evoked EPSCs with (dotted lines) or without (solid lines) γ-DGG and graph (right) (*$P = 0.0127$, *t* test; $n = 7$ to 8). (**C**) Representative voltage tracings (left) and graph (right) assessing action potential firing to a 5-ms EPSC-like somatic current (0 to 640 pA, 40-pA steps). **$P = 0.003$, χ^2 test ($n = 14$ to 17).